

Computation Set 04 Solution

AAE 440: Spacecraft Attitude Dynamics

Spring 2022

Due Date: April 13, 2022

Brendan Gillis

Problem 01: Problem Statement

Consider a satellite moving in a force-free, torque-free environment. The inertial frame and satellite body-fixed frame are represented by \mathcal{N} -frame and \mathcal{B} -frame, where $\{\hat{n}_1, \hat{n}_2, \hat{n}_3\}$ and $\{\hat{b}_1, \hat{b}_2, \hat{b}_3\}$ are right-handed vector bases fixed in \mathcal{N} -frame and \mathcal{B} -frame, respectively. The inertia tensor of the body is given by:

$$\bar{\mathbf{I}}_c = \frac{3}{4}\hat{b}_1\hat{b}_1 + \hat{b}_2\hat{b}_2 + \frac{3}{2}\hat{b}_3\hat{b}_3 \quad (\text{dimensionless}) \quad (1)$$

We consider the same initial satellite angular velocity as used in the Problem 2 of CPS3, i.e.,:

$$\boldsymbol{\omega}(t=0) = -0.1\hat{b}_1 + 0.05\hat{b}_2 + 0.1\hat{b}_3 \quad (\text{dimensionless}) \quad (2)$$

- (a): Using the function `dwdt_torqueFree` implemented in CPS3, **compute** the time history of $\boldsymbol{\omega}$ over a time span from $t = 0$ to $t = 200$ with integration tolerance 1×10^{-10} . **Show** the plots of $\omega_i(t)$ over time.
- (b): To compare the obtained numerical result against an axisymmetric case, numerically integrate the same system as in the Problem 2 of CPS3 from $t = 0$ to $t = 200$ with integration tolerance 1×10^{-10} . Denote by $\bar{\mathbf{I}}_{c,\text{axisym}}$ the inertia tensor assumed in the Problem 2 of CPS3, that is,

$$\bar{\mathbf{I}}_{c,\text{axisym}} = \hat{b}_1\hat{b}_1 + \hat{b}_2\hat{b}_2 + \frac{3}{2}\hat{b}_3\hat{b}_3 \quad (\text{dimensionless}) \quad (3)$$

Show the plots of $\omega_i(t)$ for the system with $\bar{\mathbf{I}}_{c,\text{axisym}}$ over time.

- (c): **Discuss** the qualitative differences and similarities of $\omega_i(t)$ obtained in (a) and (b) above, addressing the following points: overall behaviors (periodic? constant?), maximum/minimum values, and periods (if periodic).
- (d): The two constant integrals of motion, namely the angular momentum magnitude, $\|\mathbf{H}\|_2$, and the rotational Kinetic energy, T_{rot} , are still useful tools to check the validity of numerical simulations for general inertia bodies. Regarding the result of (a), **compute** $\|\mathbf{H}(t)\|_2$ and $T_{\text{rot}}(t)$. **Show** the plots of $\|\mathbf{H}(t)\|_2$ and $T_{\text{rot}}(t)$, and **confirm** that they are indeed constant over time.
- (e): We learned in class that there are three additional constant integrals of motion that can be found from the analogy to undamped Duffing equations. Repeating the equations in the lecture slides, the constants are given by:

$$C_i = \dot{\omega}_i^2 + A_i\omega_i^2 + \frac{B_i}{2}\omega_i^4 \quad \text{for } i = 1, 2, 3, \quad (4)$$

where A_i and B_i are constants that depend on the initial condition and $\bar{\mathbf{I}}_c$, given by:

$$\begin{aligned} A_1 &= \frac{(I_1 - I_2)(2I_3T_{\text{rot}} - \|\mathbf{H}\|_2^2) + (I_3 - I_1)(\|\mathbf{H}\|_2^2 - 2I_2T_{\text{rot}})}{I_1I_2I_3} & B_1 &= \frac{2(I_1 - I_2)(I_1 - I_3)}{I_2I_3} \\ A_2 &= \frac{(I_2 - I_3)(2I_1T_{\text{rot}} - \|\mathbf{H}\|_2^2) + (I_1 - I_2)(\|\mathbf{H}\|_2^2 - 2I_3T_{\text{rot}})}{I_1I_2I_3} & B_2 &= -\frac{2(I_1 - I_2)(I_2 - I_3)}{I_1I_3} \\ A_3 &= \frac{(I_3 - I_1)(2I_2T_{\text{rot}} - \|\mathbf{H}\|_2^2) + (I_2 - I_3)(\|\mathbf{H}\|_2^2 - 2I_1T_{\text{rot}})}{I_1I_2I_3} & B_3 &= \frac{2(I_1 - I_3)(I_2 - I_3)}{I_1I_2} \end{aligned}$$

Compute the constants C_i in Eq. (4) over time for the result of (a), **show** the plots of C_i as functions of t , and **confirm** that they are indeed constant over time.

(Hint: $\dot{\omega}_i$ in Eq. (4) can be computed by using the Euler's equations of motion given $\omega_i(t)$)

- (f): Another way to look at the torque-free attitude motion of general inertia bodies is the Poinsot construction. According to the Poinsot construction, the angular velocity vector $\boldsymbol{\omega}(t)$ moves in a plane perpendicular to the angular momentum vector \mathbf{H} in the inertial frame (called *invariable plane*). Focusing on the case with the unsymmetric inertia tensor given in Eq. (1), let us numerically verify this argument by visualizing $\boldsymbol{\omega}(t)$ and \mathbf{H} in the inertial frame, as follows:

- (f.1): In order to visualize these quantities in the inertial frame, we also need information of the satellite orientation over time to map $\boldsymbol{\omega}(t)$ and \boldsymbol{H} from \mathcal{B} -frame to \mathcal{N} -frame. Here we use the modified Rodrigues parameter (MRP) to represent the orientation of \mathcal{B} -frame relative to \mathcal{N} -frame, and suppose that the MRP vector at $t = 0$ is evaluated as:

$$\boldsymbol{\sigma}(t = 0) = \frac{1}{3}\hat{\boldsymbol{b}}_1 + \frac{1}{3}\hat{\boldsymbol{b}}_2 + \frac{1}{3}\hat{\boldsymbol{b}}_3 \quad (5)$$

Compute $\boldsymbol{\sigma}(t)$ over a time span from $t = 0$ to $t = 200$ by numerically integrating `KDE_MRP` and `dwdt_torqueFree` simultaneously, with integration tolerance 1×10^{-10} , where the shadow-set switching is not necessary (you may perform the switching at $\|\boldsymbol{\sigma}\|_2 = 1$ if you want too). **Show** the plots of $\sigma_i(t)$ over time.

- (f.2): **Compute** ${}^{\mathcal{N}}\boldsymbol{H}(t)$, i.e., time history of \boldsymbol{H} in \mathcal{N} -frame, and **show** the plots of ${}^{\mathcal{N}}H_i(t)$ to confirm that ${}^{\mathcal{N}}H_i(t)$ are indeed constant over time.

- (f.3): **Compute** ${}^{\mathcal{N}}\boldsymbol{\omega}(t)$, and **show** the three-dimensional plot of $\boldsymbol{\omega}(t)$ and \boldsymbol{H} in \mathcal{N} -frame, where represent \boldsymbol{H} by a line that connects the origin and the point given by ${}^{\mathcal{N}}\boldsymbol{H}(t = 0)$ (showing \boldsymbol{H} only at $t = 0$ is sufficient since ${}^{\mathcal{N}}\boldsymbol{H}(t)$ is time-invariant). Visually **confirm** that $\boldsymbol{\omega}(t)$ is indeed confined in a plane perpendicular to \boldsymbol{H} in \mathcal{N} -frame, where include at least two different views of the three-dimensional plot: a view that illustrates the perpendicularity of the invariable plane to \boldsymbol{H} and a view that projects the locus of $\boldsymbol{\omega}(t)$ on the invariable plane (called *herpolhode*).

- (g): Let us compare the herpolhode curve obtained in (f) against the one for an axisymmetric inertia case. To do this, **repeat** the procedure in (f.1)-(f.3) using $\bar{\bar{\mathbf{I}}}_{c,\text{axisym}}$ given in Eq. (3) with the same initial conditions Eqs. (2) and (5). **Discuss** the comparison of the two herpolhode curves obtained in (f) and in this question (e.g., are the curves circular? closed?).

Problem 01: Problem Solution

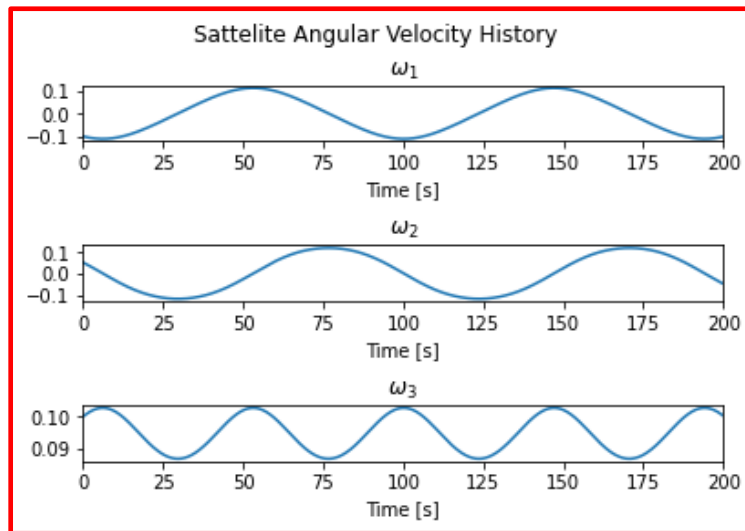
Part (a):

Using our function **dwdt_torqueFree()** we can numerically integrate this system given initial angular velocity and the inertia tensor in the \mathcal{B} frame.

```
# Problem 1
# Part a
I1 = 3/4
I2 = 1
I3 = 3/2

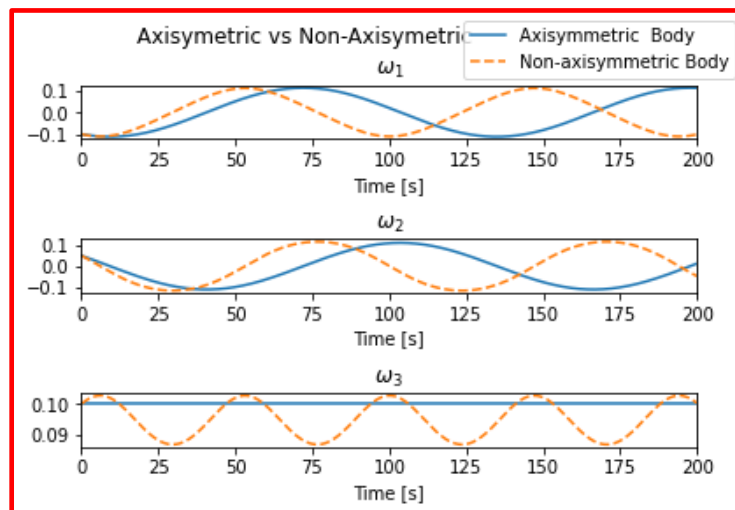
omega0 = np.array([-0.1, 0.05, 0.1])
tf = 200
t = np.linspace(0, tf, 1000)
sol = solve_ivp(sattelite_orientation_omega, y0=omega0, t_span=(0,tf),
               t_eval=t, args=(I1, I2, I3), atol=1e-10, rtol=1e-10)
t = sol.t
omega_hist = sol.y
```

```
def sattelite_orientation_omega(t, omega, I1, I2, I3):
    """
    Return the derivative of omega for
    sattelite orientation.
    """
    omega_dot = dwdt_torqueFree(omega, [I1, I2, I3])
    return omega_dot
```



Part (b):

Using the same code as in Part (a) we can compute the angular velocity of the axisymmetric body and compare it to the non-axisymmetric geometry.



Part (c):

Comparing the two results we can see that the non-axisymmetric body has a variable and periodic ω_3 compared to the axisymmetric body's constant ω_3 . Additionally, the periodic frequency of oscillation for ω_1 and ω_2 is higher in the non-axisymmetric case. Lastly, we can compare the peak values for the angular velocity noticing that for the non-axisymmetric body ω_2 and ω_3 have larger maximums.

	$\omega_{1,max}$	$\omega_{2,max}$	$\omega_{3,max}$
Axisymmetric Body	0.112	0.112	0.1
Non-Axisymmetric Body	0.11	0.117	0.103

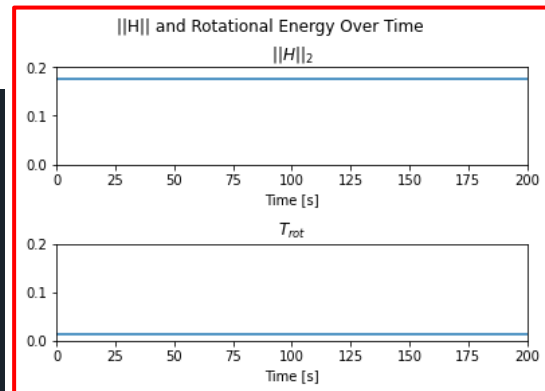
Part (d):

We can compute the magnitude of the angular momentum, and the rotation energy of the satellite by using the equations below. Using the graphs, we can confirm that both quantities are constant over time, this is something we expect for a body in a torque free environment.

$$\|H\|_2 = \|\mathcal{B}\bar{\mathbf{I}}\boldsymbol{\omega}\|_2, \quad T_{rot} = \frac{1}{2}\boldsymbol{\omega}^T\bar{\mathbf{I}}\boldsymbol{\omega}$$

```
# Part d
I = np.array([[3/4, 0, 0],
              [0, 1, 0],
              [0, 0, 3/2]])
T_rot = np.zeros_like(t)
H = np.zeros_like(omega_hist)
H_12 = np.zeros_like(t)

for i, omega in enumerate(omega_hist.transpose()):
    H[:, i] = np.dot(I, omega)
    H_12[i] = np.linalg.norm(H[:, i])
    T_rot[i] = 1/2 * np.dot(omega, H[:, i])
```



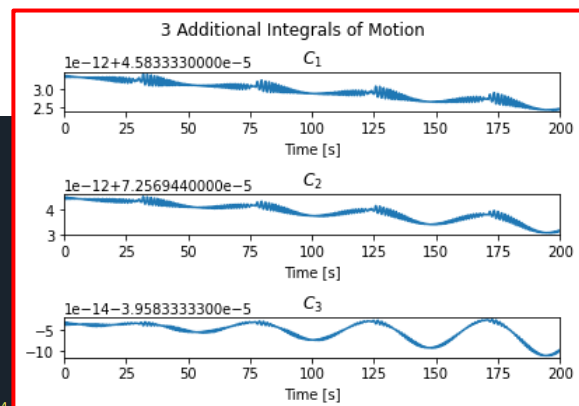
Part (e):

Using our $\boldsymbol{\omega}$ history we can compute the $\dot{\boldsymbol{\omega}}$ history with our `dwdt_torqueFree()` function. This can then be used to calculate our constants. Looking at the graph we can see that C_i is constant (axis scaled by $1e-12$) with the only variation being numerical error.

```
# Part e
A = np.zeros(3)
B = np.zeros(3)
C = np.zeros_like(omega_hist)
Trot = T_rot[5]
H = H_12[5]
A[0] = ((I1-I2)*(2*I3*Trot-H**2)+(I3-I1)*(H**2-2*I2*Trot))/(I1*I2*I3)
A[1] = ((I2-I3)*(2*I1*Trot-H**2)+(I1-I2)*(H**2-2*I3*Trot))/(I1*I2*I3)
A[2] = ((I3-I1)*(2*I2*Trot-H**2)+(I2-I3)*(H**2-2*I1*Trot))/(I1*I2*I3)
B[0] = 2*(I1-I2)*(I1-I3)/(I2*I3)
B[1] = -2*(I1-I2)*(I2-I3)/(I1*I3)
B[2] = 2*(I1-I3)*(I2-I3)/(I1*I2)

omega_dot = np.zeros_like(omega_hist)
for i, omega in enumerate(omega_hist.transpose()):
    omega_dot[:, i] = dwdt_torqueFree(omega, [I1, I2, I3])

for i, _ in enumerate(A):
    C[i, :] = omega_dot[i, :]**2 + A[i]*omega_hist[i, :]**2 + B[i]/2*omega_hist[i, :]**4
```



Part (f):

Part (f.1):

To compute the MRP history we can construct a state variable and compute its derivative:

$$\mathbf{x} = \begin{bmatrix} \boldsymbol{\omega} \\ \boldsymbol{\sigma} \end{bmatrix}, \quad \dot{\mathbf{x}} = \begin{bmatrix} \dot{\boldsymbol{\omega}} \\ \dot{\boldsymbol{\sigma}} \end{bmatrix} = \begin{bmatrix} \text{dwdt_torqueFree}(\boldsymbol{\omega}, \mathbf{I}) \\ \text{KDE_MRP}(\boldsymbol{\sigma}, \boldsymbol{\omega}) \end{bmatrix}$$

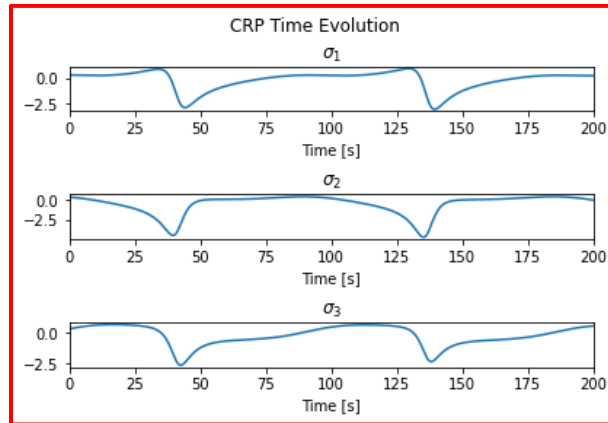
```
# Part f
state0 = np.zeros(6)
MRP0 = np.array([1/3, 1/3, 1/3])
omega0 = np.array([-0.1, 0.05, 0.1])
state0[0:3] = omega0
state0[3:6] = MRP0

tf = 200
t = np.linspace(0, tf, 1000)
sol = solve_ivp(satellite_orientation_MRP, y0=state0, t_span=(0,tf),
                t_eval=t, args=(I1, I2, I3), atol=1e-10, rtol=1e-10)

t = sol.t
omega_hist = sol.y[0:3, :]
MRP_hist = sol.y[3:6, :]

def satellite_orientation_MRP(t, state, I1, I2, I3):
    """
    Return the derivative of omega and
    MRP for satellite orientation.
    **note state is an array of [omega, MRP]
    """
    state_dot = np.zeros_like(state)
    omega = state[0:3]
    MRP = state[3:6]

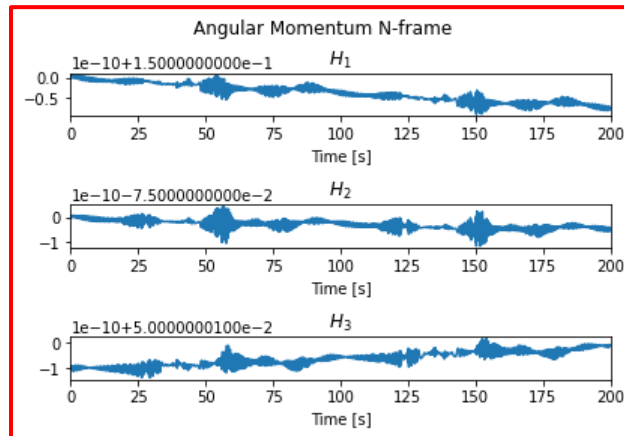
    omega_dot = dwdt_torqueFree(omega, [I1, I2, I3])
    MRP_dot = KDE_MRP(MRP, omega)
    state_dot[0:3] = omega_dot
    state_dot[3:6] = MRP_dot
    return state_dot
```



Part (f.2):

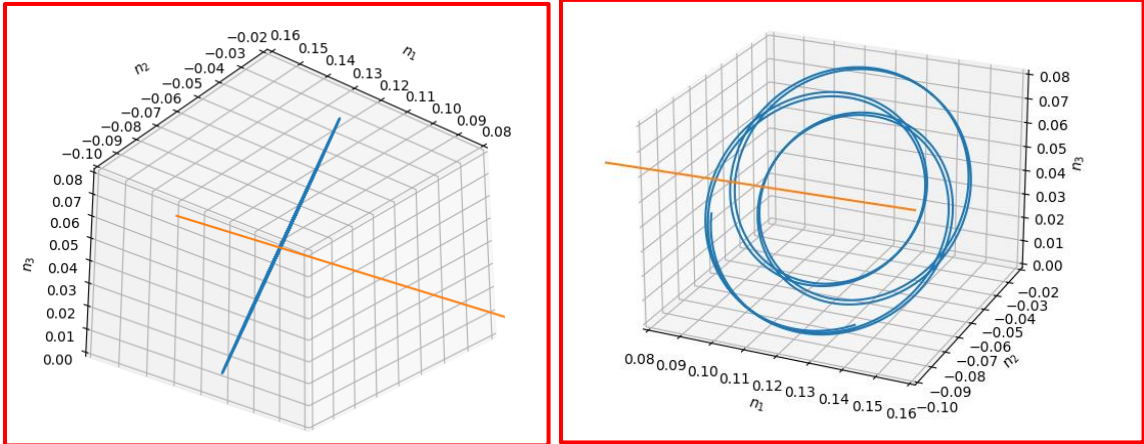
With our MRP history, we can compute the DCM $[\mathcal{N}\mathcal{B}] = [\mathcal{B}\mathcal{N}]^T$ and finally compute our angular momentum in the \mathcal{N} frame. Notice that the values are constant and only vary $O(1e-10)$ due to numerical integration error.

$${}^{\mathcal{N}}\mathbf{H} = [\mathcal{B}\mathcal{N}]^T \mathbf{H}$$



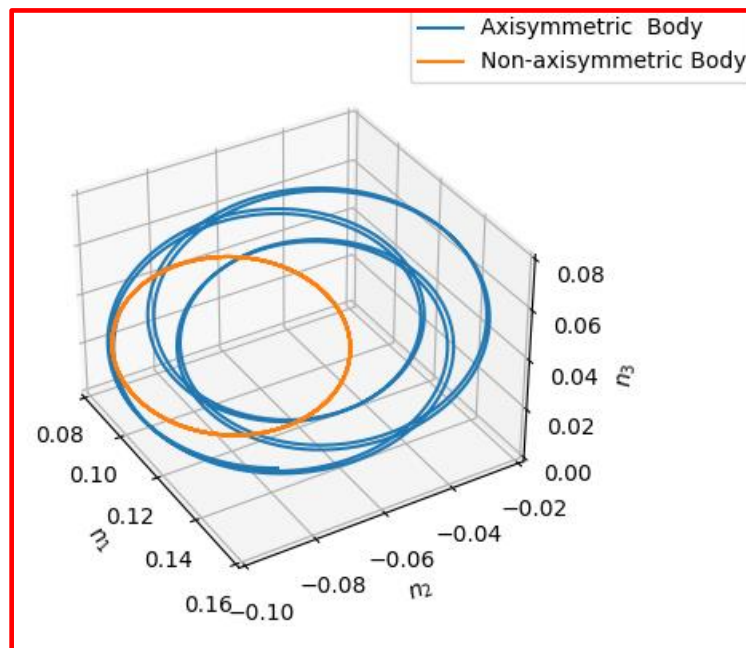
Part (f.3):

Finally, we can plot our angular velocity in the N frame with our N frame angular momentum and visually confirm that the angular momentum vector is perpendicular to the herpolhode which projects the locus of $\omega(t)$.



Part (g):

When comparing the herpolhode of the axisymmetric body to that of the non-symmetric body we can see 2 main differences. Firstly the two plains do not coincide. This makes sense because the changes between the Inertia tensors implies they do not have the same angular momentum vector, and thus not the same perpendicular plane. Additionally, the symmetric body has a simple closed circular loop while the asymmetric body has a more complex and open loop.



Problem 02: Problem Statement

This problem is concerned with numerically verifying the instability of the rotation about the intermediate moment axis. In class, we learned that the Euler's rotational equations of motion without torque (Eq. (7)) have the following three particular solutions:

$$\begin{cases} \omega_2(t) = \omega_3(t) = 0, & \omega_1(t) = \omega_{1_0} (\neq 0) & \cdots \text{Solution 1} \\ \omega_3(t) = \omega_1(t) = 0, & \omega_2(t) = \omega_{2_0} (\neq 0) & \cdots \text{Solution 2} \\ \omega_1(t) = \omega_2(t) = 0, & \omega_3(t) = \omega_{3_0} (\neq 0) & \cdots \text{Solution 3} \end{cases} \quad (6)$$

Recall that the Euler's rotational equations of motion in a torque-free environment is given as follows:

$$\begin{cases} \dot{\omega}_1 = -\frac{I_3 - I_2}{I_1} \omega_2 \omega_3 \\ \dot{\omega}_2 = -\frac{I_1 - I_3}{I_2} \omega_3 \omega_1 \\ \dot{\omega}_3 = -\frac{I_2 - I_1}{I_3} \omega_1 \omega_2 \end{cases} \quad (7)$$

Answer the following questions assuming the inertia tensor given by Eq. (1).

- (a): **Show** that each of the particular solutions in Eq. (6) indeed satisfies the differential equations Eq. (7).
- (b): **Discuss** which of the particular solutions in Eq. (6) corresponds to the maximum-energy, minimum-energy, and intermediate-energy rotational states, respectively.
- (c): Let us also numerically confirm that Eq. (6) are the particular solutions of Eq. (7). Consider the following three cases for the initial angular velocity vectors:

$$\begin{cases} \omega(t=0) = 0.1 \hat{b}_1 & \cdots \text{Case 1} \\ \omega(t=0) = 0.1 \hat{b}_2 & \cdots \text{Case 2} \\ \omega(t=0) = 0.1 \hat{b}_3 & \cdots \text{Case 3} \end{cases} \quad (\text{dimensionless}) \quad (8)$$

For each case in Eq. (8), **compute** $\omega(t)$ by numerically integrating Eq. (7) from $t = 0$ to $t = 200$ with integration tolerance 1×10^{-10} . **Show** the plots of $\omega_i(t)$ for each of the three cases, and **confirm** that the results are consistent with Eq. (6).

- (d): Now, let us consider a small perturbation in $\omega(t=0)$ for each of the three cases in Eq. (8). Specifically, we consider the following perturbed angular velocity at $t = 0$:

$$\begin{cases} \omega(t=0) = 0.1 \hat{b}_1 + 0.001 \hat{b}_2 + 0.001 \hat{b}_3 & \cdots \text{Case 1'} \\ \omega(t=0) = 0.001 \hat{b}_1 + 0.1 \hat{b}_2 + 0.001 \hat{b}_3 & \cdots \text{Case 2'} \\ \omega(t=0) = 0.001 \hat{b}_1 + 0.001 \hat{b}_2 + 0.1 \hat{b}_3 & \cdots \text{Case 3'} \end{cases} \quad (\text{dimensionless}) \quad (9)$$

- (d.1): For each case in Eq. (9), **compute** $\omega(t)$ over a time span from $t = 0$ to $t = 200$ with integration tolerance 1×10^{-10} . **Show** the plots of $\omega_i(t)$ over time.

- (d.2): **Discuss** the numerical results obtained in the previous question, addressing the following points:

- how $\omega_i(t)$ behaves over time for each case
- how $\omega_i(t)$ compares against the unperturbed results (i.e., results obtained in (b)) for each case; does the perturbation grow over time or stay around the same level? why?
- which of the maximum-energy, minimum-energy, and intermediate-energy rotational states corresponds to the unstable case

- (d.3): **Optional** (extra credit for *both* AAE 440 and 590 sections):

Show the three-dimensional herpolhode plots for each of the perturbed cases in Eq. (9), and **discuss** the results (assume the same initial condition as Eq. (5)).

Problem 02: Problem Solution

Part (a):

To confirm the solutions given by Eq. (6) are valid we can plug them into Eq. (7).

Solution 1: $\omega_2(t) = \omega_3(t) = 0$, $\omega_1(t) = \omega_{1_0} (\neq 0)$

$$\begin{cases} \dot{\omega}_1 = -\frac{I_3 - I_2}{I_1} \omega_2 \omega_3 = -\frac{I_3 - I_2}{I_1} 0 = 0 \\ \dot{\omega}_2 = -\frac{I_1 - I_3}{I_2} \omega_3 \omega_1 = -\frac{I_1 - I_3}{I_2} 0 \omega_1 = 0 \\ \dot{\omega}_3 = -\frac{I_2 - I_1}{I_3} \omega_1 \omega_2 = -\frac{I_2 - I_1}{I_3} \omega_1 0 = 0 \end{cases}$$

Solution 2: $\omega_3(t) = \omega_1(t) = 0$, $\omega_2(t) = \omega_{2_0} (\neq 0)$

$$\begin{cases} \dot{\omega}_1 = -\frac{I_3 - I_2}{I_1} \omega_2 \omega_3 = -\frac{I_3 - I_2}{I_1} 0 \omega_2 = 0 \\ \dot{\omega}_2 = -\frac{I_1 - I_3}{I_2} \omega_3 \omega_1 = -\frac{I_1 - I_3}{I_2} 0 = 0 \\ \dot{\omega}_3 = -\frac{I_2 - I_1}{I_3} \omega_1 \omega_2 = -\frac{I_2 - I_1}{I_3} \omega_2 0 = 0 \end{cases}$$

Solution 3: $\omega_1(t) = \omega_2(t) = 0$, $\omega_3(t) = \omega_{3_0} (\neq 0)$

$$\begin{cases} \dot{\omega}_1 = -\frac{I_3 - I_2}{I_1} \omega_2 \omega_3 = -\frac{I_3 - I_2}{I_1} 0 \omega_3 = 0 \\ \dot{\omega}_2 = -\frac{I_1 - I_3}{I_2} \omega_3 \omega_1 = -\frac{I_1 - I_3}{I_2} 0 \omega_3 = 0 \\ \dot{\omega}_3 = -\frac{I_2 - I_1}{I_3} \omega_1 \omega_2 = -\frac{I_2 - I_1}{I_3} 0 = 0 \end{cases}$$

Part (b):

Here we know that the maximum energy solution corresponds to Solution 1, where all angular momentum is about the \hat{b}_1 axis which has the lowest moment of inertia. On the flipside, the minimum energy solution is Solution 3, where all angular velocity and momentum is about the \hat{b}_3 axis, the axis with the highest moment of inertia. Lastly our intermediate energy solution is Solution 2 where all angular momentum is about the \hat{b}_2 axis which has a moment of inertia somewhere between the other two axis. This relationship between moment of inertia and energy makes sense because for a given angular momentum because while $\|H\|_2 = \|\mathcal{B}^T \mathbf{I} \boldsymbol{\omega}\|_2$ is constant, $T_{rot} = \frac{1}{2} \boldsymbol{\omega}^T \mathbf{I} \boldsymbol{\omega}$ will increase as the MOI decreases and $\boldsymbol{\omega}$ increases.

Part (c):

As can be seen in the graphs below, we have confirmed that are solutions are consistent with Part (a) and Part (b), noticing that when two ω_{i_0} are zero, they remain at zero, while the third angular velocity remains constant, fixed at the initial value.

```

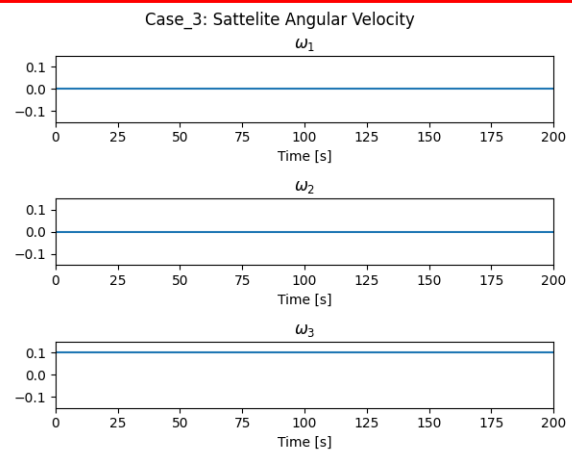
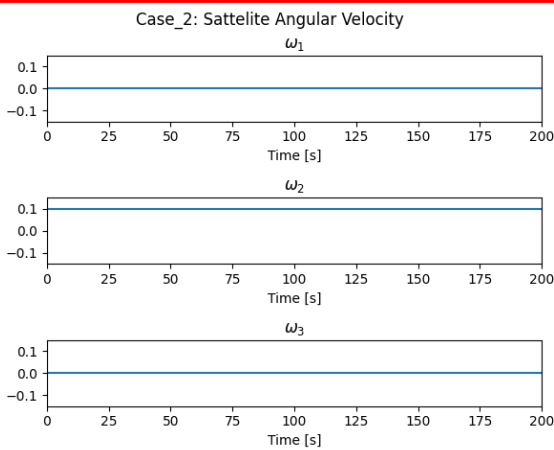
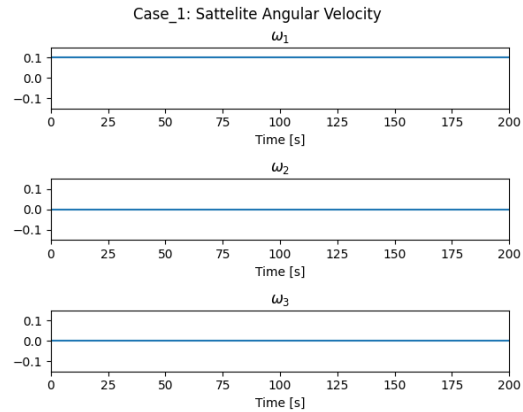
# Problem 02
# Part c
I1 = 3/4
I2 = 1
I3 = 3/2

cases = {
    "Case_1": np.array([0.1, 0, 0]),
    "Case_2": np.array([0, 0.1, 0]),
    "Case_3": np.array([0, 0, 0.1]),
    "Case_1'": np.array([0.1, 0.001, 0.001]),
    "Case_2'": np.array([0.001, 0.1, 0.001]),
    "Case_3'": np.array([0.001, 0.001, 0.1])
}

tf = 200
t = np.linspace(0, tf, 1000)

for case_num in cases:
    omega0 = cases[case_num]
    sol = solve_ivp(satellite_orientation_omega, y0=omega0, t_span=(0,tf),
                    t_eval=t, args=(I1, I2, I3), atol=1e-10, rtol=1e-10)
    t = sol.t
    omega_hist = sol.y

```

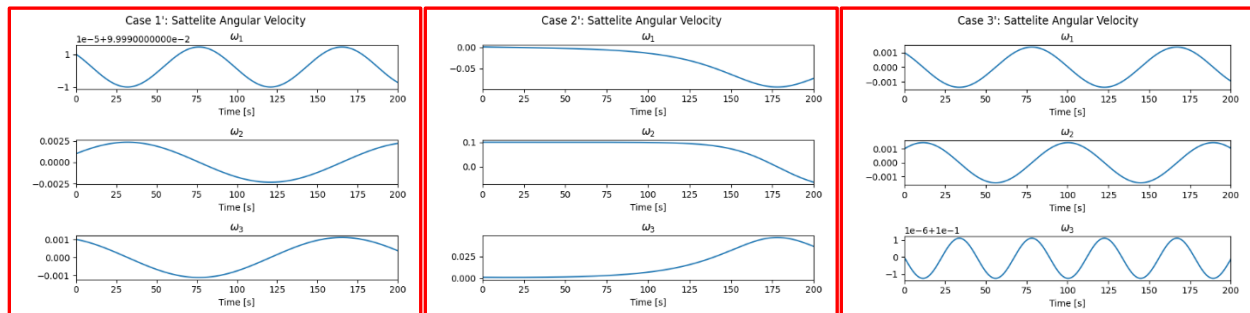


Part (d):

Note: I am using the I values from Problem 01: $I_1 = \frac{3}{4}, I_2 = 1, I_3 = \frac{3}{2}$

Part (d.1):

Using the same code as in Part (c) we can integrate this perturbed initial conditions.



Part (d.2):

Here we see that Case 1' and Case 3' remain stable and merely oscillate about their respective unperturbed solutions (notice the scaled axis). On the other hand, Case 2' appears unstable, with the initial perturbation growing over time without demonstrating any periodicity. This unstable state is associated with the intermediate-energy rotation which is notoriously unstable.

Part (d.3):

Here we can superimpose the momentum ellipsoid and energy sphere. We know the solution must lie on the intersection of these two spheres. For Case 1' and Case 3' this intersection forms a very small circle around their corresponding H_i axis indicating why the solutions shown above oscillate around the Case 1 (minimum energy) and Case 3 (maximum energy) solutions respectively. Additionally, the intermediate energy solution (Case 2) has a large and non-circular intersection between the two bodies where the solution may lie. This is what prevents the system from being stable under perturbation such as in Case 2'.

$$H^2 = H_1^2 + H_2^2 + H_3^2$$
$$1 = \frac{H_1^2}{2I_1T_{rot}} + \frac{H_2^2}{2I_2T_{rot}} + \frac{H_3^2}{2I_3T_{rot}}$$

